ACS Photonics

pubs.acs.org/journal/apchd5

Article

Color-Tunable Mixed-Cation Perovskite Single Photon Emitters

Marianna D'Amato,[#] Qi Ying Tan,[#] Quentin Glorieux, Alberto Bramati,* and Cesare Soci*

Cite This: *ACS Photonics* 2023, 10, 197−205

Read Online

ACCESS | Metrics & More | Article Recommendations | Supporting Information

ABSTRACT: Quantum photonics technologies, like wavelength division multiplexing (WDM), for high-rate quantum key distribution require narrowband, spectrally tunable single photon emitters. Physical methods that rely on the application of large mechanical strain to epitaxial quantum dots or electric and magnetic fields to color centers in 2D metal dichalcogenides provide limited spectral tunability. Here we adopt a chemical approach to synthesize a family of colloidal mixed-cation perovskite quantum dots ($Cs_{1-x}FA_xPbBr_3$) that show highly photostable, compositionally tunable single photon emission at room temperature, spanning more than 30 nm in the visible wavelength spectral range. We find that tailoring the stoichiometry of the organic formamidinium (FA) cation in all-inorganic cesium lead bromide ($CsPbBr_3$) perovskite quantum dots detunes the electronic band structure while preserving their excellent single photon emission characteristics. We argue that the mixed-cation perovskite quantum dots studied in this work offer a new platform for the realization of color-tunable single photon emitters that could be readily integrated in a diversity of quantum photonic devices.

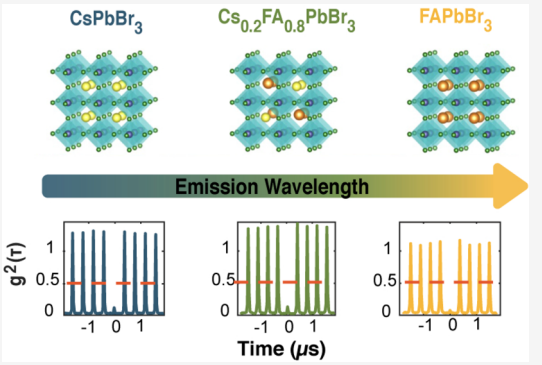

KEYWORDS: *quantum dots, mixed-cation perovskites, single photon emission, color tunability*

INTRODUCTION

The development of solid-state single photon emitters such as color centers in 2D transition metal dichalcogenides and diamond or III−V and halide perovskite colloidal quantum dots (QDs) is paving the way to quantum photonic technologies operating at room temperature. Spectral tunability of such single photon emitters is highly sought for advanced applications such as wavelength division multiplexing (WDM) for quantum key distribution. Conventional methods to achieve color-tunability of single photon emitters rely on the application of external perturbations like mechanical strain, electric, and magnetic fields. In 2019, Xia and co-workers achieved a 31 meV (equivalent to 9 nm) tunability range around 2.088 eV by applying an electric field.[1] At that point in time, the tunability range of these emitters was already an order of magnitude greater than the state-of-art of electrically tuned color center single photon emitters. Grosso and co-workers then demonstrated a spectrally tunable range of 6 meV around 2.145 eV (equivalent to 1.6 nm) by applying strain.[2] However, these techniques are hardly scalable and yield small spectral shifts even for large, applied strain and electric or magnetic fields.[2−4] Therefore, alternative color-tunable single photon systems with broader spectral tunability are highly sought.

In recent years, lead halide perovskites have attracted wide interest for their outstanding optoelectronic properties. Owing to their facile solution-processability, compositional tunability, high absorption, photoluminescence efficiency, and excellent charge transport characteristics,[5−9] perovskites have proven to be an outstanding material platform for solar cells, light-emitting devices, and laser applications.[5,10−13] In the past decade, considerable efforts were made to extend the use of halide perovskites to the domain of quantum optics. In 2015, Park and co-workers demonstrated the first ever perovskite-based single photon emission using all-inorganic $CsPbI_3$ quantum dots, revealing strong antibunching emission at room temperature, which arises from the fast nonradiative Auger recombination.[14] However, the emitters were limited by photobleaching and blinking. Since then, single photon emission from various all-inorganic cesium lead halide $CsPbX_3$ (X = Cl, Br, I) and hybrid organic−inorganic formamidinium lead halides $FAPbX_3$ quantum dots has been extensively studied to search for the most suitable single photon emitter for applications in quantum information sciences and metrology.[15−17] To date, perovskite quantum dot-based single photon emitters exhibit bright, narrow linewidth, and strong antibunching at room temperature.[18,19] Notably, Yoshimura and co-workers have shown single photon emission from $CsPb(Br/I)_3$ quantum dots during an anion exchange process, providing a first demonstration of color-tunable perovskite single photon emission.[20] Recently,

Received: September 14, 2022
Published: January 5, 2023

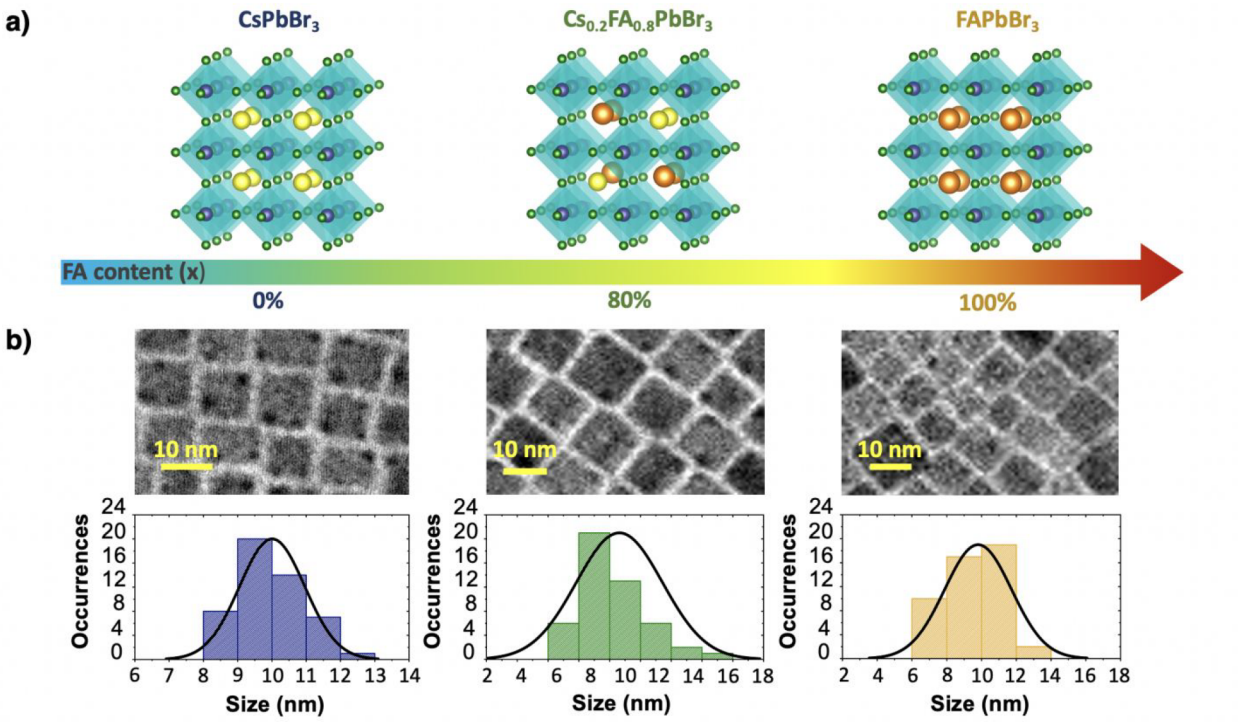

Figure 1. Compositionally tunable $Cs_{1-x}FA_xPbBr_3$quantum dots (x = 0, 0.8, and 1). (a) Changes in the crystallographic structures of the $Cs_{1-x}FA_xPbBr_3$ quantum dots with the addition of the organic FA cation additives. (b) Transmission electron microscopy images of the $CsPbBr_3$ (blue), $Cs_{0.2}FA_{0.8}PbBr_3$ (green), and $FAPbBr_3$ (yellow) quantum dots alongside their respective size distribution histograms. A sampling size of 50 quantum dots was recorded for each composition.

integration of perovskite single photon emitters into various scalable solid-state platforms was also demonstrated, confirming their potential for integrated quantum devices.[21]

Spectral tunability of perovskite quantum dots can be easily achieved by tuning their size and composition, without the need to apply mechanical strain or external fields. While mixed-halide perovskite quantum dots offer a wide compositional tunability of the emission spectrum, they are susceptible to ion segregation upon continuous illumination. The resulting luminescence instability makes them unsuitable as single photon emitters.[22] On the other hand, by modifying the composition of the A-site cations, we were able to tune the emission wavelength of the quantum dots over a relatively broad range while maintaining good photostability.[23] This concept was successfully employed in photovoltaic and light-emitting devices, yielding promising efficiency and brightness.[24−27] Alongside the color-tunability, mixed-cation perovskites bring about an enhancement in structural stability that further translates into better emission stability. As such, mixed-cation perovskites are undertaken as a common approach to overcome the "perovskite red wall", that is, the difficulty in obtaining stable red and near-infrared photoluminescence (PL).[28] Specifically, the addition of FA cation additives into $CsPbI_3$ shows an enhancement in emission stability compared to $CsPbI_3$.

By extending the compositionally tunable mixed cation perovskite approach down to the single photon level, here we look into an alternative color-tunable single photon emission system with potentially broader spectral tunability compared to conventional color-tunable single photon emitters. We demonstrate that the addition of an organic FA cation additive into all-inorganic $CsPbBr_3$ quantum dots can be used to fine-tune the emission wavelength across more than 30 nm in the visible, while retaining excellent single photon characteristics. The wide spectral tunability of $Cs_{1-x}FA_xPbBr_3$ perovskite single photon emitters, which does not require the application of mechanical strain or external fields, may facilitate their integration in quantum photonic systems, such as Bragg cavities, in which some of the emitters in a quantum dot ensemble would be at resonance or may enable applications that require wavelength division multiplexing, such as high-rate quantum key distribution.

RESULTS AND DISCUSSION

Compositionally Tunable $Cs_{1-x}FA_xPbBr_3$ Perovskite Quantum Dots. In this work, $Cs_{1-x}FA_xPbBr_3$ quantum dots were synthesized following a wet chemical approach (see SI.2 and SI.3 of the Supporting Information). Figure 1a illustrates the substitution of the inorganic Cs cation present in the crystallographic structure of $CsPbBr_3$ with the addition of the organic FA cation additive. This substitution can be achieved by varying the molar mass of formamidinium bromide (FABr) and cesium bromide (CsBr) precursors during the synthesis. Changes in the crystallographic structure with the addition of the FA cations are observed in the X-ray diffraction measurements and high-resolution transmission electron microscopy (TEM; see Figures S1 and S2 of the Supporting Information). The TEM images of the synthesized $Cs_{1-x}FA_xPbBr_3$ quantum dots (x = 0, 0.8 and 1) are shown in Figure 1b. The stoichiometry ratio x = 0.8, in particular, refers to the fraction of the FA content present in the precursor solution. The quantum dots are monodispersed and cubic shaped with an average size of (10 ± 1) nm for x = 0, (11 ± 3) nm for x = 0.8, and (10 ± 2) nm for x = 1. No significant alteration to the shape and size of synthesized quantum dots is

https://doi.org/10.1021/acsphotonics.2c01437
ACS Photonics 2023, 10, 197−205

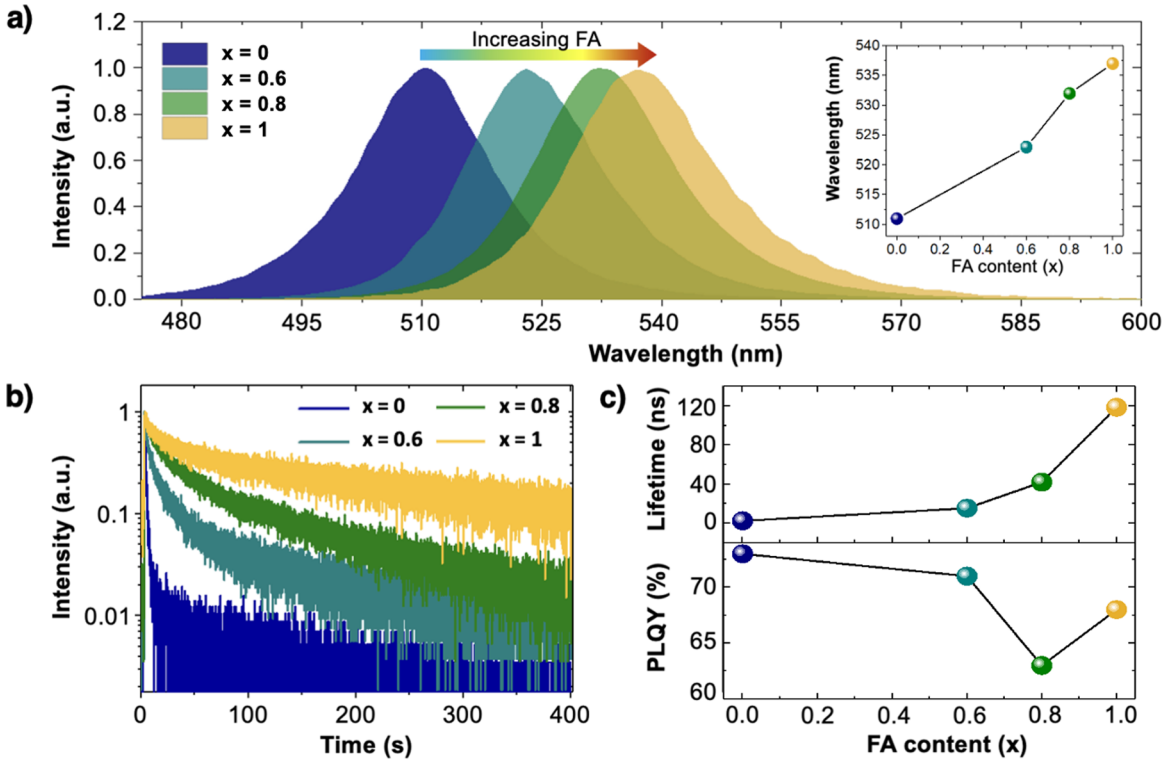

Figure 2. Spectral tunability of the $Cs_{1-x}FA_xPbBr_3$ quantum dot ensembles (x = 0, 0.6, 0.8, and 1). (a) Normalized PL spectra of the $CsPbBr_3$ (blue), $Cs_{0.4}FA_{0.6}PbBr_3$ (cyan), $Cs_{0.2}FA_{0.8}PbBr_3$ (green), and $FAPbBr_3$ (yellow) quantum dot ensembles. The insert illustrates the shift in the CEW with the different amount of FA content. (b) Time-resolved PL lifetime measurements of the $Cs_{1-x}FA_xPbBr_3$ quantum dot. (c) Changes in the average lifetime (upper panel) and PLQY (lower panel) with the different amount of FA content.

observed when the Cs cations are substituted with the FA additives. This suggests that the quantum size effect and dimensionality will not play a substantial role in the alteration of their optical properties. Small size quantum dots with radius comparable to the excitonic Bohr radius (7 nm for $CsPbBr_3$[5] and 8 nm for $FAPbBr_3$[29]) are found in the respective size distribution histograms, indicating the presence of mixed-cation $Cs_{1-x}FA_xPbBr_3$ quantum dots which should be subject to quantum confinement effects and therefore feasible for single photon generation.

Spectral Tunability of $Cs_{1-x}FA_xPbBr_3$ Quantum Dot Ensembles. To investigate the effect of FA additives on the optical properties of the quantum dots, photoluminescence measurements were performed on $Cs_{1-x}FA_xPbBr_3$ quantum dot ensembles (x = 0, 0.6, 0.8, and 1). Figure 2a shows the dependence of the PL spectra on addition of the FA cation additives. A red shift in the central emission wavelength (CEW), from 511 nm (x = 0) to 523 nm (x = 0.6), 532 nm (x = 0.8), and 537 nm (x = 1) can be clearly observed. The modification of the emission wavelength can be attributed to changes in the Pb−Br bond lengths and angles in the $PbBr_6^{4-}$ octahedron when Cs cations are substituted with FA. As the valence and conduction bands originate from the Br 4p and Pb 6p orbits, respectively, the modification of Pb−Br bond lengths and angles alters the electronic band structure of the quantum dots.[23] The full width half-maximum (FWHM) of 19 nm (x = 0 and 0.6), 20 nm (x = 0.8), and 21 nm (x = 1) may be due to inhomogeneous size distribution, electron−phonon coupling, and spatial or compositional inhomogeneity of the ensemble. These steady-state PL measurements demonstrate the possibility of controlling and fine-tuning the emission wavelength of $Cs_{1-x}FA_xPbBr_3$ quantum dot ensembles via chemical engineering.

The PL kinetics of mixed-cation perovskite quantum dot ensembles is shown in Figure 2b. The time-resolved PL measurements also reveal a clear dependence of the average lifetime of the quantum dots on the addition of the FA cation additives (Figure 2c, upper panel). The average lifetime was estimated to increase from 2.3 ns (x = 0) to 15.3 ns (x = 0.6), 42.0 ns (x = 0.8), and 118.7 ns (x = 1) by fitting the PL decays with a tri-exponential function (refer to the fitting parameters in Table S1 of the Supporting Information). The increment in the lifetime with the increase of the FA/Cs ratio is consistent with thermal mixing of states with optically forbidden transitions.[30,31] The observed correlation between the lifetime and the emission FWHM, both increasing with FA/Cs ratio, could therefore be attributed to the effect of exciton−phonon coupling due to a combination of electron−hole and electron−phonon interactions. Notably, the $Cs_{1-x}FA_xPbBr_3$ quantum dots show a high PLQY of 63−73%, regardless of their relative cation composition (Figure 2c, lower panel). Thus, addition of the FA cations does not cause a significant reduction of the quantum dot brightness.

Spectral Tunability of $Cs_{1-x}FA_xPbBr_3$ Single Photon Emitters. By using a confocal microscope, we were able to investigate the $Cs_{1-x}FA_xPbBr_3$ quantum dots at the single particle level. In this work, we focus on $Cs_{1-x}FA_xPbBr_3$ QDs, with x = 0, 0.8, and 1 composition. Optical and quantum properties of the x = 0.6 composition are also reported in sections SIV.3 and SIV.6 of the Supporting Information. As the changes in the emission spectrum and lifetime upon addition of FA in quantum dot ensembles were attributed to intrinsic mechanisms such as the alteration of crystallographic bond

https://doi.org/10.1021/acsphotonics.2c01437
ACS Photonics 2023, 10, 197−205

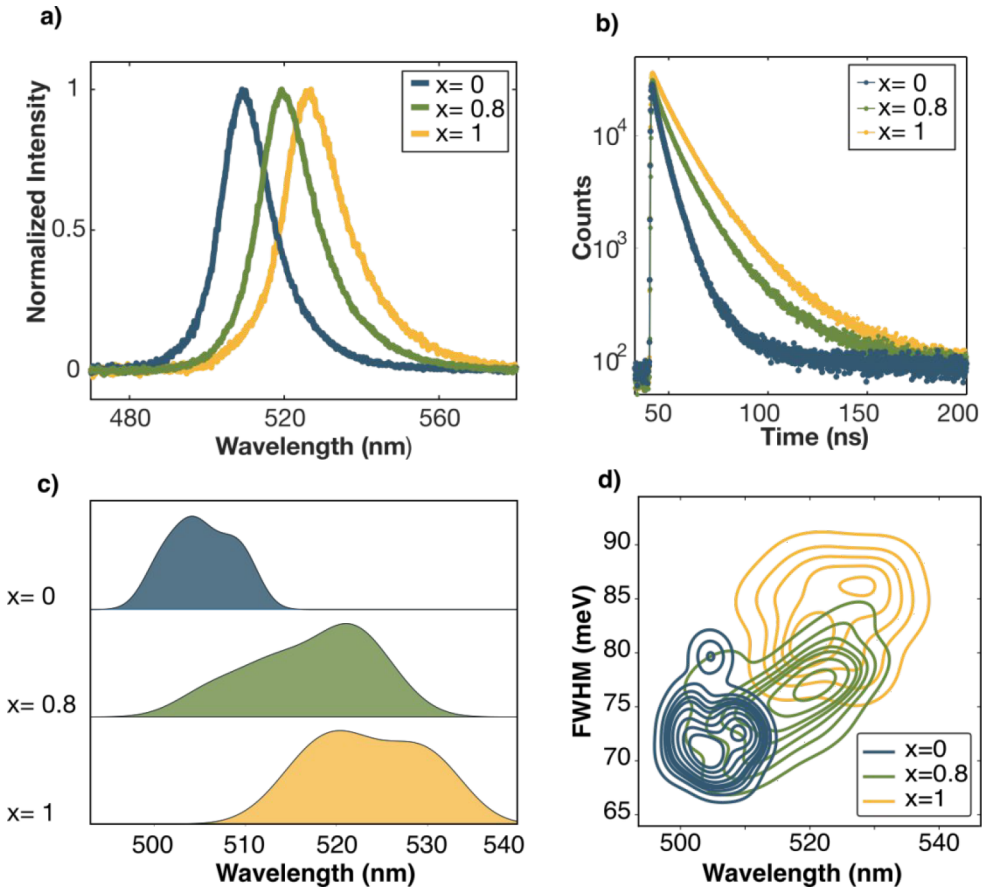

Figure 3. Spectral tunability of the $Cs_{1-x}FA_xPbBr_3$ single photon emitters (x = 0, 0.8, and 1). (a) Normalized emission spectra of an individual $CsPbBr_3$ (blue), $Cs_{0.2}FA_{0.8}PbBr_3$ (green), and $FAPbBr_3$ (yellow) quantum dot. The emission spectra are normalized to the peak intensity. (b) Typical PL decay of a $CsPbBr_3$ (blue), $Cs_{0.2}FA_{0.8}PbBr_3$ (green), and $FAPbBr_3$ (yellow) quantum dots. (c) Density distribution of the CEW for $CsPbBr_3$ (blue), $Cs_{0.2}FA_{0.8}PbBr_3$ (green), and $FAPbBr_3$ (yellow) quantum dots. A sampling size of 20 emitters for each composition was recorded. (d) Distribution of the FWHM plotted against the relative central emission wavelengths for the $CsPbBr_3$ (blue), $Cs_{0.2}FA_{0.8}PbBr_3$ (green), and $FAPbBr_3$ (yellow) emitters.

lengths and angles and the modification of the exciton recombination kinetics, compositional engineering is expected to bring about similar tunability to the optical properties of single quantum dots. Figure 3a displays the typical PL spectra of single $CsPbBr_3$, $Cs_{0.2}FA_{0.8}PbBr_3$, and $FAPbBr_3$ quantum dots, with CEW of 509, 519, and 527 nm, respectively. A red shift in the single dot PL spectra is observed upon substitution of Cs cations with FA, consistent with the trend observed in quantum dot ensembles. The spectral broadening of single quantum dot luminescence, in terms of FWHM, is 72.19 meV (~15 nm) for x = 0, 79.67 meV (~17 nm) for x = 0.8, and 87.56 meV (~19 nm) for x = 1. Likewise, an increment in the average lifetime from 5 to 36 ns is observed from typical PL decay kinetics of single $CsPbBr_3$, $Cs_{0.2}FA_{0.8}PbBr_3$, and $FAPbBr_3$ quantum dots (Figure 3b and fitting parameters in Table S2 of the Supporting Information).

To achieve statistical significance, the optical properties of 20 $Cs_{1-x}FA_xPbBr_3$ quantum dot emitters were analyzed for each composition. All the measurements were carried out at the saturation power, as explained in section IV.2 of the Supporting Information. Figure 3c shows the CEW distribution obtained for the three sets of $Cs_{1-x}FA_xPbBr_3$ quantum dots (x = 0, 0.8, and 1). The average CEWs are 505.2 ± 3.4 nm for x = 0, 517.1 ± 6.4 nm for x = 0.8, and 523.5 ± 6.0 nm for x = 1. The deviations from the average values are due to the inhomogeneous size distribution of the quantum dots. We note that the CEWs of the individual quantum dots are blue-shifted with respect to that of the corresponding ensembles, which in addition to intrinsic size inhomogeneity could be due to quantum dot size reduction upon degradation at the single-particle level. Thus, addition of FA additives allows extending the single photon emission wavelength toward the pure green, closing the single photon emission gap between pure $CsPbBr_3$ and $FAPbBr_3$ quantum dots.

Figure 3d shows the distribution of the FWHM of the PL spectra of individual $Cs_{1-x}FA_xPbBr_3$ quantum dots with representative compositions (x = 0, 0.8 and 1) plotted against their CEW. The FWHM ranges from 69.16 meV (~14 nm) to 79.78 meV (~16 nm) for x = 0, from 69.65 meV (~14.5 nm) to 82.45 meV (~18 nm) for x = 0.8, and from 78.19 meV (~17.6 nm) to 88.24 meV (~19 nm) for x = 1. By comparison with the PL line-width of quantum dot ensembles, we attribute this slightly smaller FWHM to the fact that confocal measurements target small particles in the quantum confined regime. The clear correlation between the peak wavelength and the FWHM of single dot PL seen in Figure 3d points to the crucial role of exciton confinement to achieve narrowband emission.

Photostability and Blinking of $Cs_{1-x}FA_xPbBr_3$ Single Photon Emitters. In previous studies, the performance of

https://doi.org/10.1021/acsphotonics.2c01437
ACS Photonics 2023, 10, 197−205

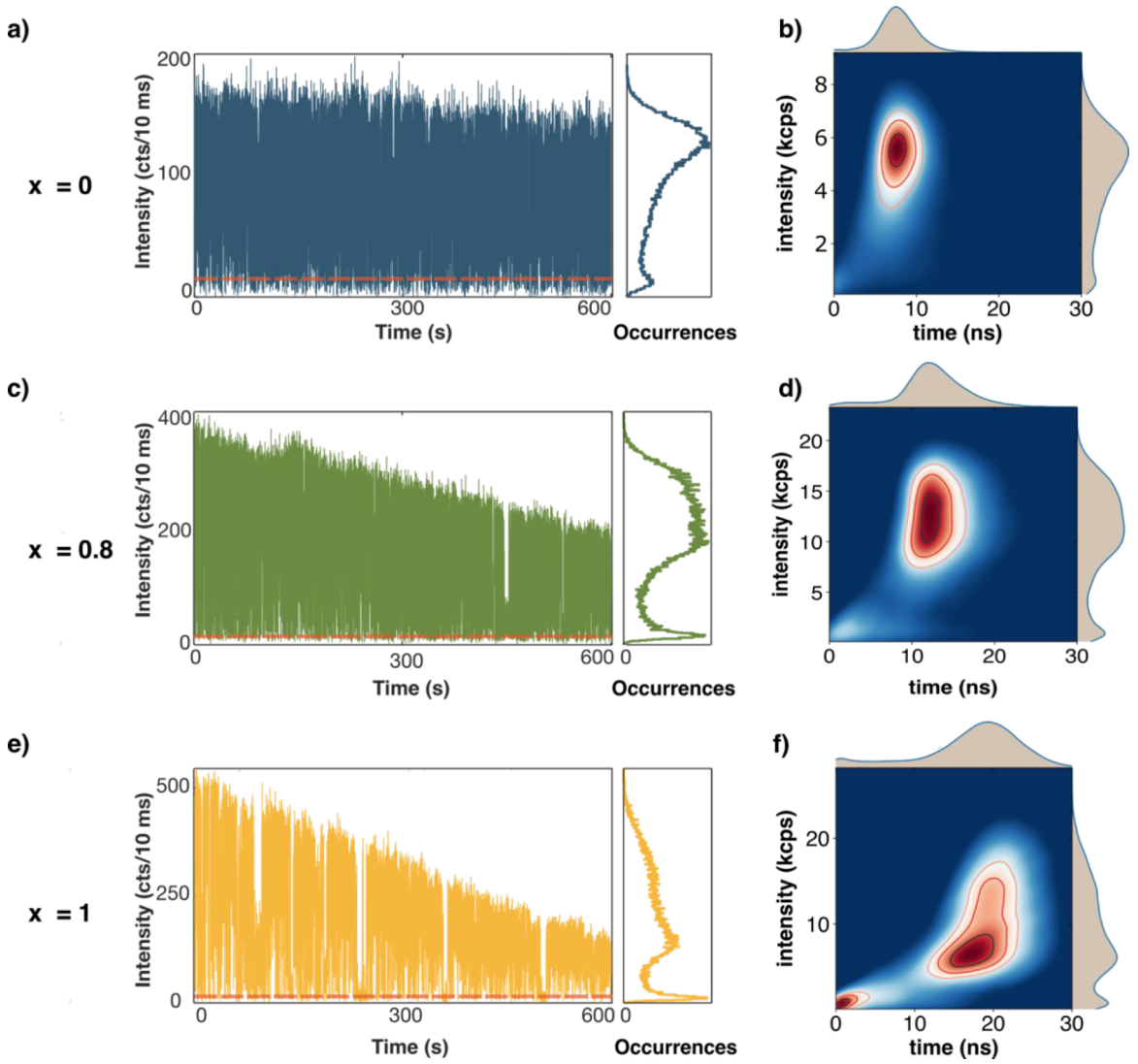

Figure 4. Photostability and blinking of $Cs_{1-x}FA_xPbBr_3$ quantum dots (x = 0, 0.8, and 1). (a, c, e) PL intensity time-traces and relative intensity histograms for single QDs with, respectively, x = 0, 0.8, and 1, with a binning time of 10 ms and an integration time of 600 s. The background level is given at 5 counts/10 ms. The threshold for the OFF states is 15 counts/10 ms (red line). (b, d, f) False color representation of FLID images for NCs with, respectively, x = 0, 0.8, and 1, obtained with a bin of 10 ms. A color change from blue to red corresponds to increasing probability of occurrences.

perovskite quantum dot devices has often been hampered by their photoinstability under illumination. In particular, irreversible photon-induced degradation and PL intermittency between the high and low intensity states, also referred as photobleaching and blinking, are frequently reported in the literature of colloidal perovskites nanocrystals.[32−35] The photostability of $Cs_{1-x}FA_xPbBr_3$ single photon emitters (x = 0, 0.8, and 1) was evaluated by measuring their PL time-traces, that is the intensity of emission as a function of time under steady-state excitation. The integration time and binning time were 600 s and 10 ms, respectively. The typical PL time-traces for individual x = 0, 0.8, and 1 quantum dots are reported in Figure 4a, c, and e. All three compositions show intermittency between the high and low emissive states, and this is corroborated by the presence of two levels in the corresponding PL intensity histograms (shown on the right of the panels). The x = 1 composition exhibits the most pronounced photoblinking compared to x = 0.8 and x = 0 samples. Moreover, under continuous illumination, a significant decrease in PL intensity is observed, with greater reduction in the case of x = 1, followed by the x = 0.8 and x = 0 perovskite quantum dots. The decrease in intensity over time is clearly manifested by the width of the PL intensity histograms, where the intensity peak is well-defined for x = 0, becomes slightly broader in the case of x = 0.8 and spreads widely for x = 1 emitters. The observed photobleaching is a typical signature of photochemical degradation of perovskites QDs.[36] The relatively higher photoinstability demonstrated in the organic−inorganic $FAPbBr_3$ (x = 1) perovskites with respect to the all-inorganic $CsPbBr_3$ (x = 0) is well reported in literature.[37]

The duration of the low intensity (OFF) periods was evaluated by thresholding the PL time traces. We selected a threshold intensity of 15 counts/10 ms, considering as OFF states the intensities below this value. We then looked at the cumulative distribution of the OFF periods P_{off} ($\tau_{off} > \tau$), which gives the probability for the emission to be OFF for a time period τ_{off} longer than a duration τ. This probability

https://doi.org/10.1021/acsphotonics.2c01437
ACS Photonics 2023, 10, 197−205

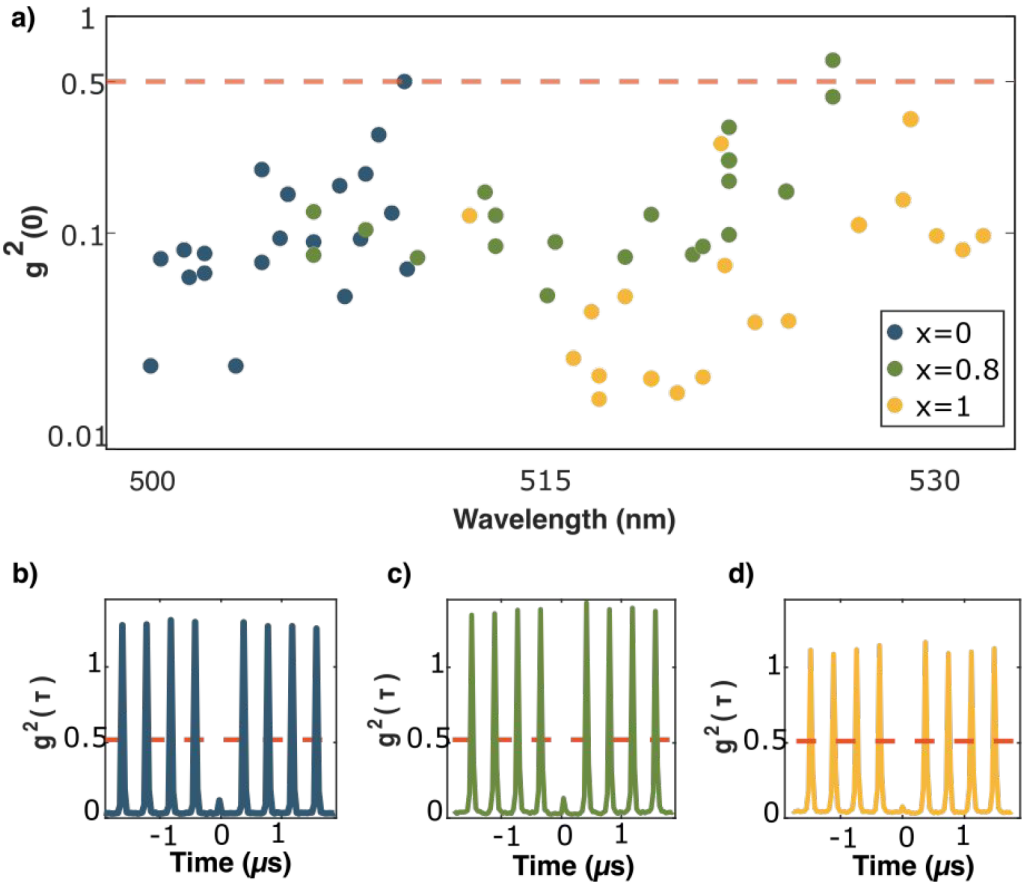

Figure 5. Tunable single photon emission of the individual $Cs_{1-x}FA_xPbBr_3$ quantum dots (x = 0, 0.8, and 1). (a) The measured $g^{(2)}(0)$ values for $CsPbBr_3$ (blue), $Cs_{0.2}FA_{0.8}PbBr_3$ (green), and $FAPbBr_3$ (yellow) in the semilogarithmic scale as a function of their CEW. A sampling size of 20 emitters per composition were taken and the threshold for antibunching is reported (red dashed line). (b–d) $g^{(2)}(\tau)$ function of an individual $Cs_{1-x}FA_xPbBr_3$ quantum dot (x = 0, 0.8, and 1).

distribution can be fitted by a power law with an exponential cutoff of the form:[38]

$$P_{off} = Ct^{-m_{off}}e^{-t/\tau_c} \quad (1)$$

where C is a constant, t refers to the time, m_{off} is the power law exponent, and τ_c is the truncation cutoff. Fitting the cumulative distribution of the OFF periods for the $Cs_{1-x}FA_xPbBr_3$ QDs with different composition, we obtain truncation cut-offs and power law exponents of τ_c = 0.25 s and m_{off} = 1.34 (x = 0), τ_c = 0.02 s, and m_{off} = 1.36 (x = 0.8) and τ_c = 0.15 s and m_{off} = 0.83 (x = 1), as shown in Figure S9 of the Supporting Information. For power law distributions with exponents smaller than 1, the so-called Levy's distributions, long OFF periods are very probable,[39] as in the case of x = 1 composition. Conversely, an exponent greater than 1 is found when long OFF periods are very unlikely and the QD blinking is reduced,[40,41] as in the case of x = 0.8 and, to a slightly lesser extent, x = 0 composition. Here, we show that using the mixed-cation perovskites to tune the single photon emission can also reduce photoinstability, assuring reduced blinking and bleaching with respect to organic–inorganic $FAPbBr_3$ (x = 1) perovskites.

To evaluate the PL intermittency more quantitatively, we analyzed the correlations between PL intensity fluctuations and PL lifetime of individual quantum dots using the fluorescence lifetime-intensity distribution (FLID) analysis (for details on the analysis method refer to SIV.5 in the Supporting Information). The correlation between these two quantities provides information on the origin of blinking in mixed-cation quantum dots. Indeed, the dependence of PL lifetime on the emitted intensity is a signature of type-A blinking, as opposed to type-B blinking,[42] where PL intensity fluctuations occur without appreciable changes in lifetime. Type-A blinking fluctuations are known to be caused by a charging/discharging mechanism: while emission from the neutral exciton state is bright, the PL yield of the charged exciton state is reduced by the opening of nonradiative channels, like nonradiative Auger decay, which compete with the radiative recombination channel and quench photon emission. FLID images obtained using a bin of 10 ms for the three QD compositions are plotted in false color, changing from blue to red with increasing probability, in Figure 4b, d, and f. The resulting FLID trajectory is a curved line, typical of type-A blinking and confirming a correlation between PL intensity and lifetime. Moreover, for the x = 0 and 0.8 emitters that showed reduced blinking the emission is found to be mostly in the bright state, while low intensity states became frequent for the x = 1 emitters, and the effect of bleaching is more pronounced. The poorer photostability of $FAPbBr_3$ quantum dots compared to the other compositions is consistent with the more prominent blue shift observed for their CEW relative to that of the ensemble.

Single Photon Emission from $Cs_{1-x}FA_xPbBr_3$ Quantum Dots. The $Cs_{1-x}FA_xPbBr_3$ quantum dots have an average size of 10 nm, with a minimum value of 7 nm (x = 0) and 6 nm

https://doi.org/10.1021/acsphotonics.2c01437
ACS Photonics 2023, 10, 197–205

(x = 0.8 and 1), as seen in Figure 1b. Given the excitonic Bohr radii of 7 nm (x = 0) and 8 nm (x = 1), quantum confinement and single photon emission, are to be expected from these quantum dots. Measurements of the second-order intensity correlation function $g^{(2)}(\tau)$ were conducted in a Hanbury Brown-Twiss configuration (Figure S6). The $g^{(2)}(\tau)$ function, which represents the probability to emit more than one photon per excitation pulse at a particular time τ, is given by

$$g^{(2)}(\tau) = \langle I(t)I(t+\tau)\rangle / \langle I(t)\rangle^2 \quad (2)$$

where t is the time, τ is the delay between two photon arrival event, and $I(t)$ and $I(\tau)$ are the PL intensities at time t and τ, respectively. At τ = 0, $g^{(2)}(0)$ approaches zero when bi- and multiexcitonic radiative recombination are highly suppressed. Figure 5a shows the $g^{(2)}(0)$ values plotted in a semilogarithmic scale as a function of their CEW. A sample size of 20 emitters were measured for each of the three compositions. We find that 97% of the emitters show $g^{(2)}(0)$ well below 0.5, a clear signature of single photon emission in all $Cs_{1-x}FA_xPbBr_3$ quantum dots. The majority of $CsPbBr_3$ (56%), $Cs_{0.2}FA_{0.8}PbBr_3$ (55%), and $FAPbBr_3$ (75%) quantum dots have $g^{(2)}(0) < 0.1$. A strong antibunching behavior has been previously reported for all-inorganic perovskites[14] and $FAPbBr_3$[17] single photon emitters and attributed to strong nonradiative Auger recombination, which effectively suppresses multiphoton emission events.[19] While 97% of the $Cs_{1-x}FA_xPbBr_3$ single photon emitters have $g^{(2)}(0) < 0.5$, we also observe emitters with $g^{(2)}(0)$ values near and above 0.5. These particular emitters tend to have longer emission wavelength relative to other emitters of the same composition. As such, one could attribute the degradation and/or loss of single photon emission (quality of the antibunching) to the larger size quantum dots, whereby quantum confinement is no longer effective. The autocorrelation functions with the best antibunching behavior recorded for each composition are shown in Figures 5b–d, yielding $g^{(2)}(0)$ values of 0.05 (x = 0), 0.04 (x = 0.8), and 0.013 (x = 1). Note that the delay peaks close to τ = 0 are higher than 1 due to the presence of blinking;[43] at large delays, when the time scale becomes comparable to the typical blinking duration, the peaks tend to 1. Thus, the value of $g^{(2)}(\tau)$ was normalized by setting the mean height of the peaks at $\tau \approx 10$ ms to be 1.[44,45] The background counts arising from the dark counts of the APDs were also subtracted as described in section SIV.7 of the Supporting Information.

CONCLUSION

In summary, we have demonstrated that the color-tunable $Cs_{1-x}FA_xPbBr_3$ quantum dot system offers an alternative approach to fine-tune the single photon emission wavelength of perovskite quantum dots via chemical engineering. This approach could not only eliminate the need of applied mechanical strain or electric and magnetic fields to control the emission spectrum but offer colloidal quantum dots with excellent single photon characteristics. With a tunability range exceeding 150 meV (~32 nm) around 2.366 eV $Cs_{1-x}FA_xPbBr_3$ perovskite single photon emitters exceed by more than 15 times the tunability range of comparable room temperature single photon emitters such as 2D TMDs. We find that addition of the second cation additive closes the gap between $CsPbBr_3$ and $FAPbBr_3$ single photon emission, while improving stability. Notably, the strong antibunching of $Cs_{0.2}FA_{0.8}PbBr_3$ quantum dots indicates single photon emission quality comparable or even higher than room temperature single photon emitters like NV defect centers in diamonds[46] or III–V semiconductor quantum dots.[47] This opens new opportunities for integration of mixed-cation perovskite quantum dots into existing quantum photonic platforms.

ASSOCIATED CONTENT

Supporting Information

The Supporting Information is available free of charge at https://pubs.acs.org/doi/10.1021/acsphotonics.2c01437.

Additional experimental details on materials and methods, as well as $Cs_{1-x}FA_xPbBr_3$ quantum dot structural characterization, ensemble, and single-particle spectroscopy (PDF)

AUTHOR INFORMATION

Corresponding Authors

Cesare Soci − *Centre for Disruptive Photonic Technologies, The Photonics Institute, 21 Nanyang Link, Nanyang Technological University, Singapore 637371, Singapore; Division of Physics and Applied Physics, 21 Nanyang Link, School of Physical and Mathematical Sciences, Nanyang Technological University, Singapore 637371, Singapore;* orcid.org/0000-0002-0149-9128; Email: csoci@ntu.edu.sg

Alberto Bramati − *Laboratoire Kastler Brossel, Sorbonne Universite, CNRS, ENS-PSL Research University, College de France, 75252 Paris, Cedex 05, France;* Email: alberto.bramati@lkb.umpc.fr

Authors

Marianna D'Amato − *Laboratoire Kastler Brossel, Sorbonne Universite, CNRS, ENS-PSL Research University, College de France, 75252 Paris, Cedex 05, France*

Qi Ying Tan − *Centre for Disruptive Photonic Technologies, The Photonics Institute, 21 Nanyang Link, Nanyang Technological University, Singapore 637371, Singapore; Interdisciplinary Graduate School, Energy Research Institute @NTU (ERI@N), Nanyang Technological University, Singapore 637553, Singapore*

Quentin Glorieux − *Laboratoire Kastler Brossel, Sorbonne Universite, CNRS, ENS-PSL Research University, College de France, 75252 Paris, Cedex 05, France*

Complete contact information is available at: https://pubs.acs.org/10.1021/acsphotonics.2c01437

Author Contributions

Q.Y.T. and C.S. conceived the idea. Q.Y.T. synthesized the perovskite QDs and characterized QD ensembles by TEM and PL measurements. Q.Y.T. measured absorption and PLQY of QD suspensions. M.D. prepared and optimized the deposition of low-density QD films, performed steady-state and time-resolved fluorescence spectroscopy at single particle level and $g^2(\tau)$ measurements with Time-Correlated Single Photon Counting (TCSPC) technique, statistical analysis of the optical properties, and characterized the blinking with Cumulative Distribution Function (CDF) and FLID analysis. Q.Y.T., M.D., A.B., and C.S. drafted the manuscript. All authors discussed the results and contributed to finalizing the

https://doi.org/10.1021/acsphotonics.2c01437
ACS Photonics 2023, 10, 197−205

manuscript. Q.G. and A.B supervised the research in LKB and C.S. supervised the research in NTU.

Author Contributions

#These authors, alphabetically ordered, contributed equally to this work.

Funding

Research in NTU was supported by the Agency for Science, Technology and Research A*STAR-AME Programmatic Grant on Nanoantenna Spatial Light Modulators for Next-Gen Display Technologies (Grant No. A18A7b0058) and the Singapore Ministry of Education MOE Tier 3 (Grant No. MOE2016-T3-1-006). Research in LKB was supported by the ANR Project IPER-Nano2 (ANR-18CE30-0023) and by the European Union's Horizon 2020 Research and Innovation Program Nanobright (No. 828972). Q.G. and A.B. are members of the Institut Universitaire de France (IUF).

Notes

The authors declare no competing financial interest.

■ ACKNOWLEDGMENTS

We thank Maciej Klein for his help with the absorption and PLQY measurements of the QD ensembles, and Dong Shuyu for her assistance with X-ray diffraction measurements of the QDs. Data supporting the findings of this study are openly available in the NTU research data repository DR-NTU at https://doi.org/10.21979/N9/DOWJDP. Additional data related to this paper may be requested from the authors.

■ REFERENCES

(1) Xia, Y.; Li, Q.; Kim, J.; Bao, W.; Gong, C.; Yang, S.; Wang, Y.; Zhang, X. Room-Temperature Giant Stark Effect of Single Photon Emitter in van der Waals Material. *Nano Lett.* **2019**, *19* (10), 7100.

(2) Grosso, G.; Moon, H.; Lienhard, B.; Ali, S.; Efetov, D. K.; Furchi, M. M.; Jarillo-Herrero, P.; Ford, M. J.; Aharonovich, I.; Englund, D. Tunable and high-purity room temperature single-photon emission from atomic defects in hexagonal boron nitride. *Nat. Commun.* **2017**, *8* (1), 705.

(3) Noh, G.; Choi, D.; Kim, J.-H.; Im, D.-G.; Kim, Y.-H.; Seo, H.; Lee, J. Stark Tuning of Single-Photon Emitters in Hexagonal Boron Nitride. *Nano Lett.* **2018**, *18* (8), 4710−4715.

(4) Stevenson, R. M.; Young, R. J.; Atkinson, P.; Cooper, K.; Ritchie, D. A.; Shields, A. J. A semiconductor source of triggered entangled photon pairs. *Nature* **2006**, *439* (7073), 179−82.

(5) Protesescu, L.; Yakunin, S.; Bodnarchuk, M. I.; Krieg, F.; Caputo, R.; Hendon, C. H.; Yang, R. X.; Walsh, A.; Kovalenko, M. V. Nanocrystals of Cesium Lead Halide Perovskites (CsPbX (3), X = Cl, Br, and I): Novel Optoelectronic Materials Showing Bright Emission with Wide Color Gamut. *Nano Lett.* **2015**, *15* (6), 3692−6.

(6) Zhang, F.; Zhong, H.; Chen, C.; Wu, X.-g.; Hu, X.; Huang, H.; Han, J.; Zou, B.; Dong, Y. Brightly Luminescent and Color-Tunable Colloidal CH3NH3PbX3 (X = Br, I, Cl) Quantum Dots: Potential Alternatives for Display Technology. *ACS Nano* **2015**, *9* (4), 4533−4542.

(7) Li, X.; Wu, Y.; Zhang, S.; Cai, B.; Gu, Y.; Song, J.; Zeng, H. CsPbX3Quantum Dots for Lighting and Displays: Room-Temperature Synthesis, Photoluminescence Superiorities, Underlying Origins and White Light-Emitting Diodes. *Adv. Funct. Mater.* **2016**, *26* (15), 2435−2445.

(8) Park, N.-G. Organometal Perovskite Light Absorbers Toward a 20% Efficiency Low-Cost Solid-State Mesoscopic Solar Cell. *J. Phys. Chem. Lett.* **2013**, *4* (15), 2423−2429.

(9) Herz, L. M. Charge-Carrier Mobilities in Metal Halide Perovskites: Fundamental Mechanisms and Limits. *ACS Energy Letters* **2017**, *2* (7), 1539−1548.

(10) Min, H.; Lee, D. Y.; Kim, J.; Kim, G.; Lee, K. S.; Kim, J.; Paik, M. J.; Kim, Y. K.; Kim, K. S.; Kim, M. G.; Shin, T. J.; Il Seok, S. Perovskite solar cells with atomically coherent interlayers on SnO2 electrodes. *Nature* **2021**, *598* (7881), 444−450.

(11) Yakunin, S.; Protesescu, L.; Krieg, F.; Bodnarchuk, M. I.; Nedelcu, G.; Humer, M.; De Luca, G.; Fiebig, M.; Heiss, W.; Kovalenko, M. V. Low-threshold amplified spontaneous emission and lasing from colloidal nanocrystals of caesium lead halide perovskites. *Nat. Commun.* **2015**, *6*, 8056.

(12) Shamsi, J.; Rainò, G.; Kovalenko, M. V.; Stranks, S. D. To nano or not to nano for bright halide perovskite emitters. *Nat. Nanotechnol.* **2021**, *16* (11), 1164.

(13) Roman, B. J.; Sheldon, M. The role of mid-gap states in all-inorganic CsPbBr3 nanoparticle one photon up-conversion. *Chem. Commun.* **2018**, *54* (50), 6851.

(14) Park, Y.-S.; Guo, S.; Makarov, N. S.; Klimov, V. I. Room Temperature Single-Photon Emission from Individual Perovskite Quantum Dots. *ACS Nano* **2015**, *9* (10), 10386−10393.

(15) Utzat, H.; Sun, W.; Kaplan, A. E. K.; Krieg, F.; Ginterseder, M.; Spokoyny, B.; Klein, N. D.; Shulenberger, K. E.; Perkinson, C. F.; Kovalenko, M. V.; Bawendi, M. G. Coherent single-photon emission from colloidal lead halide perovskite quantum dots. *Science* **2019**, *363* (6431), 1068−1072.

(16) Fu, M.; Tamarat, P.; Trebbia, J. B.; Bodnarchuk, M. I.; Kovalenko, M. V.; Even, J.; Lounis, B. Unraveling exciton-phonon coupling in individual $FAPbI_3$ nanocrystals emitting near-infrared single photons. *Nat. Commun.* **2018**, *9* (1), 3318.

(17) Trinh, C. T.; Minh, D. N.; Ahn, K. J.; Kang, Y.; Lee, K.-G. Organic-Inorganic FAPbBr3 Perovskite Quantum Dots as a Quantum Light Source: Single-Photon Emission and Blinking Behaviors. *ACS Photonics* **2018**, *5* (12), 4937−4943.

(18) Rainò, G.; Yazdani, N.; Boehme, S. C.; Kober-Czerny, M.; Zhu, C.; Krieg, F.; Rossell, M. D.; Erni, R.; Wood, V.; Infante, I.; Kovalenko, M. V. Ultra-narrow room-temperature emission from single $CsPbBr_3$ perovskite quantum dots. *Nat. Commun.* **2022**, *13* (1), 2587.

(19) Zhu, C.; Marczak, M.; Feld, L.; Boehme, S. C.; Bernasconi, C.; Moskalenko, A.; Cherniukh, I.; Dirin, D.; Bodnarchuk, M. I.; Kovalenko, M. V.; Raino, G. Room-Temperature, Highly Pure Single-Photon Sources from All-Inorgnic Lead Halide Perovskite Quantum Dots. *Nano Lett.* **2022**, *22* (9), 3751−3760.

(20) Yoshimura, H.; Yamauchi, M.; Masuo, S. In Situ Observation of Emission Behavior during Anion-Exchange Reaction of a Cesium Lead Halide Perovskite Nanocrystal at Single-Nanocrystal Level. *J. Phys. Chem.* **2020**, *11*, 530−535.

(21) Pierini, S.; D'Amato, M.; Goyal, M.; Glorieux, Q.; Giacobino, E.; Lhuillier, E.; Couteau, C.; Bramati, A. Highly Photostable Perovskite Nanocubes: Toward Integrated Single Photon Sources Based on Tapered Nanofibers. *ACS Photonics* **2020**, *7* (8), 2265−2272.

(22) Knight, A. J.; Borchert, J.; Oliver, R. D. J.; Patel, J. B.; Radaelli, P. G.; Snaith, H. J.; Johnston, M. B.; Herz, L. M. Halide Segregation in Mixed-Halide Perovskites: Influence of A-Site Cations. *ACS Energy Letters* **2021**, *6* (2), 799.

(23) Chen, D.; Chen, X.; Wan, Z.; Fang, G. Full-Spectral Fine-Tuning Visible Emissions from Cation Hybrid Cs1-mFAmPbX3 (X = Cl, Br, and I, 0 < /= m < /= 1) Quantum Dots. *ACS Appl. Mater. Interfaces* **2017**, *9* (24), 20671−20678.

(24) Hazarika, A.; Zhao, Q.; Gaulding, E. A.; Christians, J. A.; Dou, B.; Marshall, A. R.; Moot, T.; Berry, J. J.; Johnson, J. C.; Luther, J. M. Perovskite Quantum Dot Photovoltaic Materials beyond the Reach of Thin Films: Full-Range Tuning of A-Site Cation Composition. *ACS Nano* **2018**, *12* (10), 10327−10337.

(25) Zhang, Y.-W.; Wu, G.; Dang, H.; Ma, K.; Chen, S. Multicolored Mixed-Organic-Cation Perovskite Quantum Dots (FAxMA1-xPbX3, X = Br and I) for White Light-Emitting Diodes. *Ind. Eng. Chem. Res.* **2017**, *56* (36), 10053−10059.

(26) Hao, M.; Bai, Y.; Zeiske, S.; Ren, L.; Liu, J.; Yuan, Y.; Zarrabi, N.; Cheng, N.; Ghasemi, M.; Chen, P.; Lyu, M.; He, D.; Yun, J.-H.;

Du, Y.; Wang, Y.; Ding, S.; Armin, A.; Meredith, P.; Liu, G.; Cheng, H.-M.; Wang, L. Ligand-assisted cation-exchange engineering for high-efficiency colloidal Cs1-xFAxPbI3 quantum dot solar cells with reduced phase segregation. *Nature Energy* **2020**, *5* (1), 79−88.
(27) Zhang, X.; Liu, H.; Wang, W.; Zhang, J.; Xu, B.; Karen, K. L.; Zheng, Y.; Liu, S.; Chen, S.; Wang, K.; Sun, X. W. Hybrid Perovskite Light-Emitting Diodes Based on Perovskite Nanocrystals with Organic-Inorganic Mixed Cations. *Adv. Mater.* **2017**, *29* (18).1606405
(28) Protesescu, L.; Yakunin, S.; Kumar, S.; Bar, J.; Bertolotti, F.; Masciocchi, N.; Guagliardi, A.; Grotevent, M.; Shorubalko, I.; Bodnarchuk, M. I.; Shih, C. J.; Kovalenko, M. V. Dismantling the "Red Wall" of Colloidal Perovskites: Highly Luminescent Formamidinium and Formamidinium-Cesium Lead Iodide Nanocrystals. *ACS Nano* **2017**, *11* (3), 3119−3134.
(29) Perumal, A.; Shendre, S.; Li, M.; Tay, Y. K. E.; Sharma, V. K.; Chen, S.; Demir, H. V.; et al. High brightness formamidinium lead bromide perovskite nanocrystal light emitting devices. *Sci. Rep.* **2016**, *6* (1), 1−10.
(30) Krieg, F.; Sercel, P. C.; Burian, M.; Andrusiv, H.; Bodnarchuk, M.; Stöferle, T.; Mahrt; Naumenko, D.; Amenitsch, H.; Raino, G.; Kovalenko, M. Monodisperse Long-Chain Sulfobetaine-Capped CsPbBr3 Nanocrystals and Their Superfluorescent Assemblies. *ACS Cent. Sci.* **2021**, *7* (1), 135.
(31) Tamarat, P.; Bodnarchuk, M. I.; Trebbia, J. B.; et al. The ground exciton state of formamidinium lead bromide perovskite nanocrystals is a singlet dark state. *Nat. Mater.* **2019**, *18*, 717−724.
(32) Efros, A. L.; Nesbitt, D. J. Origin and control of blinking in quantum dots. *Nat. Nanotechnol.* **2016**, *11* (8), 661−671.
(33) Frantsuzov, P.; Kuno, M.; Janko, B.; Marcus, R. A. Universal emission intermittency in quantum dots, nanorods and nanowires. *Nat. Phys.* **2008**, *4* (7), 519−522.
(34) Bradac, C.; Gaebel, T.; Naidoo, N.; Sellars, M. J.; Twamley, J.; Brown, L. J.; Barnard, A. S.; Plakhotnik, T.; Zvyagin, A. V.; Rabeau, J. R. Observation and control of blinking nitrogen-vacancy centres in discrete nanodiamonds. *Nat. Nanotechnol.* **2010**, *5* (5), 345−349.
(35) Gensch, T.; Böhmer, M.; Aramendía, P. F. Single molecule blinking and photobleaching separated by wide-field fluorescence microscopy. *J. Phys. Chem. A* **2005**, *109* (30), 6652−6658.
(36) An, R.; Zhang, F.; Zou, X.; Tang, Y.; Liang, M.; Oshchapovskyy, I.; Zheng, K.; et al. Photostability and photodegradation processes in colloidal $CsPbI_3$ perovskite quantum dots. *ACS Appl. Mater. Interfaces* **2018**, *10* (45), 39222−39227.
(37) Ahmad, Z.; Najeeb, M. A.; Shakoor, R. A.; Alashraf, A.; Al-Muhtaseb, S. A.; Soliman, A.; Nazeeruddin, M. K. Instability in $CH_3NH_3PbI_3$ perovskite solar cells due to elemental migration and chemical composition changes. *Sci. Rep.* **2017**, *7* (1), 1−8.
(38) Chung, I.; Bawendi, M. G. Relationship between single quantum-dot intermittency and fluorescence intensity decays from collections of dots. *Phys. Rev. B* **2004**, *70*, 165304.
(39) Brokmann, X.; Hermier, J. P.; Messin, G.; Desbiolles, P.; Bouchaud, J. P.; Dahan, M. Statistical aging and nonergodicity in the fluorescence of single nanocrystals. *Physical review letters* **2003**, *90* (12), 120601.
(40) Mahler, B.; Spinicelli, P.; Buil, S.; Quelin, X.; Hermier, J. P.; Dubertret, B. Towards non-blinking colloidal quantum dots. *Nature materials* **2008**, *7* (8), 659−664.
(41) Pisanello, F.; Leménager, G.; Martiradonna, L.; Carbone, L.; Vezzoli, S.; Desfonds, P.; Bramati, A.; et al. Non-blinking single-photon generation with anisotropic colloidal nanocrystals: towards room-temperature, efficient, colloidal quantum sources. *Adv. Mater.* **2013**, *25* (14), 1974−1980.
(42) Galland, C.; Ghosh, Y.; Steinbrück, A.; Sykora, M.; Hollingsworth, J. A.; Klimov, V. I.; Htoon, H. Two types of luminescence blinking revealed by spectroelectrochemistry of single quantum dots. *Nature* **2011**, *479* (7372), 203−207.
(43) Manceau, M.; Vezzoli, S.; Glorieux, Q.; Giacobino, E.; Carbone, L.; De Vittorio, M.; Hermier, J.-P.; Bramati, A. CdSe/CdS Dot-in-Rods Nanocrystals Fast Blinking Dynamics. *ChemPhysChem* **2018**, *19* (23), 3288−3295.
(44) Pierini, S; D'Amato, M; Joos, M; Glorieux, Q; Giacobino, E; Lhuillier, E; Couteau, C; Bramati, A Hybrid devices for quantum nanophotonics. *Journal of Physics: Conference Series* **2020**, *1537* (1), 012005.
(45) Manceau, M.; Vezzoli, S.; Glorieux, Q.; Pisanello, F.; Giacobino, E.; Carbone, L.; De Vittorio, M.; Bramati, A. Effect of charging on CdSe/CdS dot-in-rods single-photon emission. *Phys. Rev. B* **2014**, *90* (3), 035311.
(46) Kurtsiefer, C.; Mayer, S.; Zarda, P.; Weinfurter, H. Stable solid-state source of single photons. *Physical review letters* **2000**, *85* (2), 290.
(47) Wang, X.; Xu, L.; Jiang, Y.; Yin, Z.; Chan, C. C.; Deng, C.; Taylor, R. A. III-V compounds as single photon emitters. *Journal of Semiconductors* **2019**, *40* (7), 071906.

https://doi.org/10.1021/acsphotonics.2c01437
ACS Photonics 2023, 10, 197−205